DR. GUSTAVO MENDONCA (Orcid ID : 0000-0003-2290-4046)

Article type : Original Article



# Hydrophilic titanium surface modulates early stages of osseointegration in osteoporosis

**Rafael Amorim Cavalcanti de Siqueira**[1], DDS, MSc, PhD.
**Jessica Afonso Ferreira**[2,3], DDS, MSc, PhD.
**Fábio Antônio Piola Rizzante**[4], DDS, MSc., PhD.
**Guilherme Faria Moura**[2,3], DDS, MSc.
**Daniela Baccelli Silveira Mendonça**[3], DDS, MSc., PhD.
**Denildo de Magalhães**[2], DDS, PhD.
**Renata Cimões**[5], DDS, MSc., PhD.
**Gustavo Mendonça**[3*], DDS, MSc., PhD.

[1]Department of Periodontics and Oral Medicine, School of Dentistry, University of Michigan, Ann Arbor, MI, USA.
[2]Department of Periodontology and Implant Dentistry, School of Dentistry, Federal University of Uberlandia, Uberlândia, MG, Brazil.
[3]Department of Biological and Material Sciences & Prosthodontics, University of Michigan School of Dentistry, Ann Arbor, MI, USA.
[4]Department of Comprehensive Care, School of Dental Medicine, Case Western Reserve University, Cleveland, OH, USA.
[5]Department of Prosthesis and Maxillofacial Surgery, Federal University of Pernambuco, Recife, Pernambuco, Brazil.

**Corresponding author:**

**Gustavo Mendonça, DDS, MS, PhD**
**Department of Biological and Material Sciences & Prosthodontics**
**University of Michigan School of Dentistry**
**1011 North University Avenue**
**Ann Arbor, Michigan 48109-1078, USA.**
**TEL: + 1 734 763-3325**
**FAX: (734) 936-0374**
**e-mail address: mgustavo@umich.edu**

**Abstract word count: 365**
**Total word count: 3864**
**Total number of tables and figures: 8**
**Number of references: 61**

## ABSTRACT

**Objective:** Using a mouse osteoporotic model this study aimed to determine the influence of hydrophilic titanium surfaces on gene expression and bone formation during the osseointegration process.

**Background:** Based on the previous evidence, it is plausible to assume that osteoporotic bone has a different potential of bone healing. Therefore, implant surface modifications studies that aims at enhancing bone formation to further improve short- and long-term clinical outcomes in osteoporosis is necessary.

**Material and Methods:** Fifty female, 3-month old mice were included in this study. Osteoporosis was induced by ovariectomy (OVX, test group) in 25 mice. The further 25 mice had ovaries exposed but not removed (SHAM, control group). Seven weeks following the ovariectomy procedures, 1 customized implant (0.7 x 8 mm) of each surface was placed in each femur for both groups. Implants had either a hydrophobic surface (SAE) or a hydrophilic treatment surface (SAE-HD). Calcium (Ca) and Phosphorus (P) content was measured by Energy-dispersive x-ray spectroscopy (EDS) after 7 days. The femurs were analyzed for bone-to-implant contact (BIC) and bone volume fraction (BV) by Nano computed-tomography (nano-CT) after 14 and 28 days. Same specimens were further submitted to histological analysis. Additionally, after 3 and 7 days,

implants were removed and cells were collected around the implant to access gene expression profile of key osteogenic (*Runx2*, *Alp*, *Sp7*, *Bsp*, *Sost*, *Ocn*) and inflammatory genes (*IL-1β*, *IL-10*, *Tnf-α* and *Nos2*) by qRT-PCR assay. Statistical analysis was performed by ANOVA and paired *t*-test with significance at $p < 0.05$. **Results:** The amount of Ca and P deposited on the surface due to the mineralization process was higher for SAE-HD compared to SAE on the intra-group analysis. Nano CT and histology revealed more BV and BIC for SAE-HD in SHAM and OVX groups compared to SAE. Analysis in OVX group showed that most genes (i.e. *ALP*, *Runx2*) involved in the bone morphogenetic protein (BMP) signaling, were significantly activated in the hydrophilic treatment. **Conclusion:** Both surfaces were able to modulate bone responses toward osteoblast differentiation. SAE-HD presented a faster response in terms of bone formation and osteogenic gene expression compared to SAE. Hydrophilic surface in situations of osteoporosis seems to provide additional benefits in the early stages of osseointegration.

**Key-words:** osseointegration, gene expression, surface treatment, dental implant, osteoporosis

## INTRODUCTION

The number of elderly patients seeking treatment with dental implant has increased in recent years. At the same time, an increased number of these patients are expected to suffer from one or more chronic metabolic diseases, like osteoporosis, which can affect bone healing and potentially lead to more implant failures or greater marginal bone loss [1-4]. Osteoporosis is a skeletal disorder characterized by a reduction in bone mass and microarchitectural deterioration of the bone tissue that increases fracture risk, affecting 300 million people worldwide [5]. This disease is more prevalent in postmenopausal women, and it will likely increase as the overall population over 60 years old is expected to grow to nearly 2.1 billion by 2050 [6,7].

Both etiology and therapy of osteoporosis (estrogens, vitamin D, and bisphosphonates) may interfere with wound healing process and osseointegration [8-11]. *In vitro* and preclinical studies in ovariectomized animals

reported that low bone density might present negative effect on multiple situations where bone remodeling occur, such as: delay of femoral fractures healing [12], critical-sized cranial defects following grafting with alloplastic bone substitutes [13], post-extraction sockets [14-16], healing after osteotomy [16] and the osseointegration of titanium dental implants [9-11]. Osseointegration is important for determining the success of dental implant outcomes as it results in the direct structural and functional connection between the surface of a load-bearing implant and living bone [17]. Previous studies have also highlighted the importance of bone-implant contact (BIC) for long-term successful implant osseointegration [18].

Therefore, the modification of the titanium implant surface, e.g. by the deposition of inorganic/ organic coatings, has been used to improve the implant-bone response in osteoporotic conditions compared to healthy conditions [18-25]. The positive effect of surface topography on implant osseointegration, accomplished through grit blasting and acid etching, has been previously reported [26-30]. Also, hydrophilic surfaces have been used to enhance further the bone formation process reducing the healing time in diabetic and osteoporotic conditions [31-33].

The mechanisms that control osseointegration are only partially understood and more studies are required in situations of poor bone quality and impaired healing. Activation and de-activation of key regulatory genes is crucial to the process of differentiation of osteoprogenitor cells and it is also affected by cell-surface interactions [34]. In osteoporosis, the proliferation and recruitment of mesenchymal stem cells (MSCs) to the site of bone remodeling are impaired [35,36]. Also, MSCs have a reduced potential to differentiate into osteoblasts and an increased tendency to differentiate into adipocytes [37,38]. Based on the previous evidence, it is logical to assume that osteoporotic bone has a different bone healing potential, and therefore, a modification of the current treatment protocols and materials for dental implant therapy may be necessary when treating osteoporotic patients. The present study aims to evaluate the influence of different titanium implant surfaces (hydrophobic and hydrophilic) on osteogenic genes modulation and bone formation, in an osteoporotic mouse model.

## 2. MATERIAL AND METHODS

### Experimental animal model

The research protocol was approved by The Institutional Animal Use & Care Committee (IACUC), University of Michigan. This research was conducted in compliance with University guidelines, State and Federal regulations and the standards of the "Guide for the Care and Use of Laboratory Animals". Fifty female, 3 months old, C57BL/6 (B6) mice (Jackson laboratories), weighting between 22 and 30 g, with no injuries or congenital defects were used in this study. Before the surgery, animals were anaesthetized via inhalation of 4-5% isoflurane (Piramal, Pennsylvania, USA) for induction and maintained with 1-3% of isoflurane as needed to maintain surgical anesthesia using a calibrated vaporizer. Level of anesthesia was monitored by toe pinch and eye reflex. Ophthalmic ointment was used to protect the animals' eyes during surgery. Alcohol-soaked gauze sponges were alternated with iodophor-soaked gauze sponges or Q-tips to disinfect the surgical site. The wound area was shaved gently. The surgical field was cleaned with povidone iodine solution (alternating scrubs of povidone iodine/chlorhexidine with normal saline/alcohol/sterile water). For post-operative pain management, Carprofen (Piramal, Pennsylvania, USA) was provided preemptively and for 48 hours postoperatively. Signs of complications related to surgery were monitored daily. Surgery records were kept and also included frequency of post-operative analgesics administered.

### Induction of osteoporosis-like conditions

Experimental osteoporosis was induced by ovariectomy (OVX) and calcium and phosphorus deficient diet using a method previously described [14]. For all animals, the ovaries were identified and displayed bilaterally, following a longitudinal incision in the region below the last rib and next to the kidney. In 25 OVX animals (OVX, test group), hemostasis was secured by suturing the top of the fallopian tube (Vicryl 4-0; Ethicon, Somerville, NJ, USA) and the ovaries together with the oviduct and a small portion of the uterus were excised. The remaining 25 mice (SHAM, control group) only had their ovaries identified and surgically exposed, and free access to regular food and water. The muscles and skin were then sutured in layers in all animals (Vicryl 4-0; Ethicon) and wound

clips were used to final closure. Ovariectomized mice were fed with calcium and phosphorus deficient diet (0.1% calcium and phosphorus 0.77%; Lab diet, St. Louis, MO, USA) and water ad libitum throughout the whole experimental period. Following the 7 weeks protocol for osteoporosis induction, a 3-D nano-CT was performed, and it was validated that OVX produced an osteoporotic phenotype in the appendicular skeleton (Fig. 1). Implant placement was standardized for both OVX and SHAM groups. Hydrophobic surface (SAE) implant was placed on left femur and hydrophilic surface (SAE-HD) implant was placed on right femur of each mouse.

**Experimental implant surgical procedure**

The same experimental surgical procedure was performed in all animals. The distal femur was accessed through a medial parapatellar arthrotomy. After locating the femoral intercondylar notch, the femoral intramedullary canal was manually reamed with a sequence from a 30-gauge needle to a 21-gauge needle. Then, a cpTi grade IV implant (diameter 0.7 mm and length 8mm) prepared with a hydrophobic (SAE) or hydrophilic (SAE-HD) surface was placed (Neodent, Curitiba, Brazil) (Fig. 2). Each femur received a different implant surface, as stated above. The soft tissues were repositioned, and the overlying muscles and periosteum were sutured with simple interrupted sutures (Vicryl 5-0; Ethicon). The animals were euthanized with an overdose of carbon dioxide at different time points.

**SEM and EDS Analysis**

Five animals for each OVX and SHAM group were euthanized at 7 days after implant placement for chemical analysis. The implants were examined by high-resolution scanning electron microscopy (Hitachi S-4700, Tokyo, Japan) and energy-dispersive x-ray spectroscopy (EDS) to identify chemical elements in several types of sample components, whether mineral or organic. The calcium and phosphorus content were measured at the surface of each implant in 6 different areas. The results were expressed by the mean value of the 6 measurements randomly taken.

**Nano CT Analysis**

Animals were euthanized at 14 and 28 days post-implant placement (n=5, per group). Muscle tissue and epiphyses were removed, and bone/implant samples were fixed with 4% paraformaldehyde (Z Fix, Anatech Ltd, Battle Creek, MI, USA). Non-destructive analysis of the neoformed bone at the implant interface was performed using Nano CT (Nanotom-S, phoenix|x-ray, GE; Germany), located at the University of Michigan, Orthopedic Research Laboratories, Ann Arbor, MI. The samples were scanned with pieces rotation in 360º, using monochromatic x-rays with 80 kV, 320µA, 120ms exposure time, 3 frame averaging, 6 µm voxel size. The software NRecon and Dataviewer were used for the image reconstruction. A region of interest (ROI) around the implant was defined, where the bone volume fraction (BV) could be calculated. Outcome variables were: BV, being the percentage of bone present in the region around the implant and BIC, being the area percentage of the total implant surface covered by bone.

**Histological processing**

Immediately following the Nano CT imaging, samples were prepared for histological assessments of non-demineralized samples. Fixation of samples was performed in 10% formaldehyde for a week followed by gradual dehydration using a series of alcohol solutions ranging from 70 to 100% ethanol. Specimens were processed using a Leica ASP300 tissue processor and then placed in a series of methyl methacrylate and dibutyl phthalate with progressively higher concentrations of benzoyl peroxide. Samples were manually embedded in partially polymerized poly methyl methacrylate (PMMA) and allowed to cure at room temperature for up to ten days. Blocks were then hardened in a 37°C oven overnight. The tissues were sliced (~300 µm in thickness) through the center of the implant along its long axis with an Isomet 2000 precision diamond saw (Buehler Ltd., Lake Bluff, Illinois, USA), glued to acrylic plates with an acrylate-based cement Techonovit 7000 VCL (Külzer, Wehrheim, Hesse, Germany), and allowed to set for 24 h prior to grinding and polishing. The sections were then reduced to a final thickness of ~30 µm by grinding/polishing using a series of abrasive papers EXACT 310 CP series (400, 1200, 55 and 15) (EXACT Apparatebau, Norderstedt, Schleswig-Holstein, Germany) under water irrigation. The unstained sections were analyzed by polarized light microscopy Axioplan 2

(Zeiss, Jena, Thuringia, Germany); the sections were then stained with toluidine blue and submitted to an optical microscopy evaluation Olympus BX51 Microscope (Olympus America Inc.).

**Histomorphometric analysis**

In each histological slice, eight non-superimposing fields, corresponding to the implant/bone interface (three fields on each side of the implant), were captured by scanning at a 4x magnification, and digital image analysis software (Zen 2.5®; Carl Zeiss Meditec, Dublin, CA) was used to measure the BIC. The regions of BIC along the implant perimeter were subtracted from the total implant perimeter, and calculations were performed to determine the final % of BIC. Results were reported as percentages.

**RNA isolation, complementary DNA (cDNA) synthesis, and quantitative real-time polymerase chain reaction (qRT-PCR)**

Five animals for each group were euthanized at 3 and 7 days for qRT-PCR analysis. Femurs were harvested, and implants were explanted by fracture of the femurs. For evaluation of gene expression in cells adherent to explanted endosseous implant surfaces, immediately following retrieval the implants were rinsed in cold PBS (Gibco-Life Technologies, Grand Island, NY, USA) and then placed into 1mL of TRIzol reagent (Invitrogen Life Technologies, Carlsbad, CA, USA). Total RNA was isolated following TRIzol manufacturer's recommendations. Total RNA concentration was quantified using a NanoDrop 2000 spectrophotometer (NanoDrop products, Wilmington, DE, USA). The extracted RNA was reverse transcribed following a conventional protocol to synthesize complementary DNA (cDNA). cDNA synthesis was performed using 500ng of RNA following the manufacturer's protocol (SuperScript VILO cDNA Synthesis, Invitrogen Life Technologies, Carlsbad, CA, USA).

Then, qRT-PCR was performed to check the expression of osteogenic markers: runt-related transcription factor-2 (*Runx-2*), transcription factor *Sp7*, also called osterix (*Sp7*), alkaline phosphatase (*Alp*), osteocalcin (*Ocn*), bone sialoprotein (*Bsp*), and sclerostin (*Sost*). Also, inflammatory related genes such as: interleukin 1 beta (*IL-1β*), interleukin 10 (*IL-10*), and tumor necrosis factor

alpha (*Tnf-*$\alpha$) were evaluated. All primers were obtained from Qiagen (Qiagen Sciences, Germantown, MD, USA). The reactions were prepared using SYBR Green Real-Time PCR Master Mix (Qiagen) according to the manufacturer's protocol. Thermal cycling was performed on an ABI 7900HT (Applied Biosystems, Foster City, CA, USA) according to recommended protocol. SHAM SAE 3 days samples were set as control; 1.0-fold expression level. Glyceraldehyde-3-phosphate dehydrogenase (*Gapdh*) was used as house-keeping control gene.

**Statistical Analysis**

qPCR data were analyzed using the $2^{-\Delta\Delta Ct}$ method and results reported as fold change [39,40]. T-test was performed for comparison of gene expression levels at days 3 and 7. Calcium and phosphorus content, NanoCT parameters (BV and BIC) and histomorphometric analysis were subjected to analysis of variance (ANOVA) followed by Tukey post hoc test to determine differences between experimental time points and implant groups. For all tests, results were considered significant if $p \leq 0.05$. For all analysis, control group was SHAM SAE 3 days.

**RESULTS**

**Surface Analysis by EDS**

The amount of calcium and phosphorus deposited on the implant surface was higher for SAE-HD surface compared to the SAE surface within SHAM and OVX groups. Calcium and phosphorus content were higher in SHAM compared to OVX mice. Statistically significant differences were observed for the amount of calcium deposition between SHAM SAE and SHAM SAE-HD, and phosphorus content between the different surfaces within SHAM and OVX groups (Figs. 3A and 3B).

**Nano CT Analysis**

Three-dimensional (3D) reconstruction of the new bone formation around the implant for the different titanium surfaces are shown in Fig. 4. The area of new bone tissue and the entire trabecular bone around implants are represented by yellow and green, respectively. At 14 days, greater BV and BIC was

observed for SAE-HD compared to SAE surface within OVX and SHAM groups (Figs. 5A and 5B). However, it reached statistically significant difference for BV (p=0.0001) and BIC (p=0.0026) between both surfaces only for SHAM animals. At 28 days, SAE-HD implant surface showed increased BV for the OVX animals compared to the other groups, with a statistically significant difference from SHAM SAE-HD groups (p=0.0001) (Fig. 5A). Similar results were noted for the OVX SAE-HD group for BIC after 28 days, with statistically significant differences between SHAM SAE (p=0.0196), SHAM SAE-HD (p=0.0132 and OVX SAE (p=0.0143) groups (Fig. 5B).

**Histological analysis**

In general, analysis of bone formation around the implants in all groups occurred in a time-dependent way, and after 28 days of implant placement a significant portion of the implant surface was in contact with newly formed bone. At 14 days after implant placement in the bone marrow, it was observed more trabecular spaces between the cortical bone and the implant surfaces for SAE surface in both SHAM and OVX groups compared to the SAE-HD surface, representing an earlier deposition of newly formed bone at the implant surface of the SAE-HD groups. (Figs. 6A-D).

At 28 days, the SHAM group with SAE surface revealed considerably less amount of BIC compared to the SHAM with SAE-HD implant, and both OVX samples (Figs. 6E-H).

**Histomorphometric results**

Values (in percentages) for BIC on the SAE and SAE-HD implants at all experimental time points are illustrated in Fig. 7. After 14 days, the SAE-HD group presented a higher BIC than did the SAE group for SHAM group, but no statistically significant differences were observed in between the groups. At day 28, both SAE and SAE-HD groups had enhanced BIC rates compared with SAE at day 14. Statistically significant differences were observed for SHAM-SAE (p=0.0163) and SHAM-SAE-HD (p=0.0238) between 14 and 28 days.

**Osteogenic Differentiation and Gene Expression**

For early osteogenic markers, there was a 2- and 2.5-fold increase for *Alp* gene at 3 and 7 days, respectively, in the OVX SAE-HD group compared to control. For *Runx2* gene expression levels, there was a 2.4-fold increase in the OVX SAE-HD group compared to the control group after 7 days. *Sp7* mRNA levels were increased by 2.7-fold and 2.4-fold for SHAM SAE and SHAM SAE-HD after 7 days, respectively. For OVX SAE and OVX SAE-HD, levels close to baseline values were observed for *Sp7* after 7 days (Fig. 8A).

Analysis of late osteogenic markers showed a 2-fold increase for *Sost* at 3 days for SHAM SAE-HD group compared to control group, while for all other time points and groups, *Sost* expression was lower than baseline levels. There was an increase of 2.8-fold for *Bsp* levels at 7 days for the SHAM groups and a 1.5- and 2.3-fold for SAE and SAE-HD in OVX, respectively. *Ocn* presented increased mRNA expression levels at 7 days for all groups compared to the control group. Comparing the osteoporotic like condition groups, there was a 1.2- and 1.6-fold increase for the SAE and SAE-HD implants, respectively. (Fig. 8B).

When evaluating the inflammatory markers, *IL-1*$\beta$ presented higher fold-expression levels for the OVX groups compared to the SHAM groups at the same time points. *IL-10* had a 1.7-fold increase for the SHAM SAE-HD at 3 days while all other groups and time points showed reduced *IL-10* expression compared to the control group. *Tnf-*$\alpha$ expression had a 1.8-fold increase for OVX SAE-HD at day 3 and a 2.2-fold increase for group OVX SAE at day 7. *Nos2* expression levels were close or below baseline levels for all groups at both time points, except for group SHAM SAE-HD that presented a 2-fold increase at 3 days (Fig. 8C).

**DISCUSSION**

In the present study, two different implant titanium surfaces were used in an approach to compare bone formation and gene expression levels in osteoporotic and control mice. Interestingly, by EDS and qRT-PCR, a significant increase in Calcium and Phosphorus, and upregulation of most genes related to osteogenesis were observed in association with the use of a hydrophilic surface

compared to a hydrophobic surface, in both osteoporotic and healthy conditions. Increased roughness and wettability of a Ti surface have been shown to induce differentiation of mesenchymal stem cells into bone forming cells, creating an osteogenic and angiogenic microenvironment [33,41]. Histological studies have also demonstrated improvements of the osseointegration process with the increase in the wettability of titanium implants surface in comparison to implants that received sandblasting and acid etching only [42,43]. In the present study, experimental osteoporosis was induced in adult female mice by bilateral ovariectomy and the administration of a calcium and phosphorus deficient diet. Successful induction of osteoporosis in rodents has been reported in previous studies [14,44]. Moreover, a recent study demonstrated an evident osteoporotic phenotype in both long bones and alveolar bone of mice by induction of osteoporosis via ovariectomy [45].

In the present report, it was observed greater amount of calcium and phosphorus around the hydrophilic surface, and it is known from previous studies that $Ca^{2+}$ and $(PO_4)^{3-}$ ions stimulate cellular and intracellular signaling and favor osteoblastic cell activity in the process of bone formation [46,47]. Further, $Ca^{2+}$ ions might increase osteogenic cell chemotaxis and migration toward the coated surface via the activation of calcium signaling. $Ca^{2+}$ and $(PO_4)^{3-}$ ions also play a crucial role in bone mineralization and can facilitate the precipitation of bone-like apatite on the implant surface [48,49].

Preclinical studies reported lower osseointegration rates in ovariectomized animals when different types of root form implants were inserted in extraoral locations [9,11]. In addition, clinical reports suggested that implant osseointegration may be delayed and biomaterial failures may be increased in osteoporotic patients [9,10]. qRT-PCR analysis at 3 and 7 days revealed different effects of the experimental surfaces on gene expression levels involved in peri-implant osteogenesis. The hydrophilic surface often presented higher expression levels of osteogenic marker. These findings can present an important clinical implication since during the osseointegration process an early recruitment, attachment, and proliferation of bone cells to the implant surface is required [46]. A recent study [33] reported that hydrophilic implant surfaces led to earlier expression of signaling pathways associated with osteoblast differentiation as compared to hydrophobic surfaces. Similarly, the over

expression of the osteo-related genes could be related to the hydrophilic surface used in this study. *Alp* is described as a marker of primary osteogenic activity and calcification regulation [50] and its presence demonstrates possible osteoblasts differentiation and bone formation [51,52]. Furthermore, it has been recently shown [16] that alkaline phosphatase activity declines, with a comparable increase in osteoclast activity in osteoporotic conditions. The present study demonstrated a 2- and 2.5-fold increase for *Alp* at 3 and 7 days, respectively, in the OVX SAE-HD group compared to control. It can be speculated that the hydrophilic surface apparently modulated a higher expression of this gene required for optimal bone formation. *Runx2* and *Sp7* are transcription factors essential for osteoblast differentiation and their increase are an indicative of osteoinduction and osteoblast differentiation [29]. A recent published study demonstrated reduced osteoprogenitor cells in the PDL of osteoporotic mice with a significantly decrease in absolute number and percentage of cells that were *Sp7* and *Runx2* positive, after tooth extraction and during socket healing [45]. Remarkably, *Runx2* was overexpressed in OVX SAE-HD after 7 days and *Sp7* was significantly reduced in osteoporotic conditions for both surfaces, suggesting that implant surface can partially upregulate osteogenic gene expression.

Activation of the immune system controls the initial response to the implanted material and affects its long-term survival and integration [53]. On the other hand, a lack of inflammatory response will leave the debris from implantation to remain and affect the integration of the material and generation of new tissue [54]. Greater levels of pro-inflammatory factors (*IL-1*$\beta$ and *Tnf-α*) were present in comparison to anti-inflammatory factors (*IL-10* and *Nos2*) after 7 days. *Tnf-α* was higher for OVX group after 3 days for the hydrophilic surface and reduced after 7 days. Resolution of inflammation is a key event to allow osteoblast recruitment and differentiation for bone formation. The lower levels of *Tnf-α* after 7 days could not only indicate that the initial inflammatory response is about to resolve but it is also an indication of osteogenic potential at the site, as shown by the increase in *Runx2* mRNA levels. Although *Tnf-α* was demonstrated to suppress osteogenic differentiation in estrogen-deficiency induced osteoporosis, this was not observed in the present experiment [55]. Additionaly, the tested implant surfaces did not demonstrate a substantial role

specific on anti-inflammatory markers, and *IL-10* levels remained constant after 7 days.

The histological findings revealed slightly better behavior for the hydrophilic surface on new bone formation and BIC within groups comparison. Better osseointegration, often described as increased BIC, for hydrophilic implants have been demonstrated through in vivo studies [21,56,57]. However, further comparisons of implant surfaces in osteoporotic conditions are missing. Further corroborating our data, previous studies demonstrated that the use of hydrophilic surface may promote bone healing and osseointegration in osteoporotic rabbits [21]. Enhanced bone area and BIC around implants placed in sheep tibia was also demonstrated in a recent study [58]. A limitation of BV and BIC analysis throughout NanoCT measurements are the inherent artifacts surrounding high density materials such as titanium implants that degrade image quality and interfere with image interpretation. Therefore, histomorphometric analysis using histological sections was performed in order to further validate BIC values. The present study presents several limitations. Although mice are easy to handle and house, and genetically well characterized, their bone metabolism is relatively different from humans, and their bone structure is absent of Haversian system [59,60]. On the other hand, the bone metabolism and composition of larger animals are more similar to the one of humans, but the utilization of this animal model is associated with overall higher costs and ethical debates [61]. Additionally, loading features is totally different in animals compared with human beings. Data on implant loading was not tested in the present study since they cannot be transferred to clinical practice, especially in this type of animal model. Therefore, the extrapolation of the present experimental findings obtained with small animals to the clinical scenario is difficult, and further studies should investigate the extent to which modified implant surfaces can improve osseointegration in patients with compromised bone. Within the limitations of the present study, it was suggested that hydrophilic surfaces can modulate genes expressed by adjacent progenitor cells, controlling some of the initial phenomena of osseointegration.

## CONCLUSION

Our results suggest that a hydrophilic surface could be considered to improve osseointegration in the presence of osteoporosis, since an upregulation of genes related to osteogenic differentiation was observed. Furthermore, we observed significant higher amount of calcium and phosphorus content, and slightly greater BV and BIC for the hydrophilic surface even in conditions of induced osteoporosis.

## REFERENCES


1. Gaetti-Jardim EC, Santiago-Junior JF, Goiato MC, Pellizer EP, Magro-Filho O, Jardim Junior EG. Dental implants in patients with osteoporosis: a clinical reality? *J Craniofac Surg.* 2011;22(3):1111-1113.
2. Giro G, Chambrone L, Goldstein A, et al. Impact of osteoporosis in dental implants: A systematic review. *World J Orthop.* 2015;6(2):311-315.
3. Wagner F, Schuder K, Hof M, Heuberer S, Seemann R, Dvorak G. Does osteoporosis influence the marginal peri-implant bone level in female patients? A cross-sectional study in a matched collective. *Clin Implant Dent Relat Res.* 2017;19(4):616-623.
4. de Medeiros F, Kudo GAH, Leme BG, et al. Dental implants in patients with osteoporosis: a systematic review with meta-analysis. *Int J Oral Maxillofac Surg.* 2018;47(4):480-491.
5. Temmerman A, Rasmusson L, Kubler A, Thor A, Quirynen M. An open, prospective, non-randomized, controlled, multicentre study to evaluate the clinical outcome of implant treatment in women over 60 years of age with osteoporosis/osteopenia: 1-year results. *Clin Oral Implants Res.* 2017;28(1):95-102.
6. Wright NC, Looker AC, Saag KG, et al. The recent prevalence of osteoporosis and low bone mass in the United States based on bone mineral density at the femoral neck or lumbar spine. *J Bone Miner Res.* 2014;29(11):2520-2526.
7. Rachner TD, Khosla S, Hofbauer LC. Osteoporosis: now and the future. *Lancet.* 2011;377(9773):1276-1287.
8. Sanfilippo F, Bianchi AE. Osteoporosis: the effect on maxillary bone resorption and therapeutic possibilities by means of implant prostheses--a literature review

and clinical considerations. *Int J Periodontics Restorative Dent.* 2003;23(5):447-457.

9. Fini M, Giavaresi G, Greggi T, et al. Biological assessment of the bone-screw interface after insertion of uncoated and hydroxyapatite-coated pedicular screws in the osteopenic sheep. *J Biomed Mater Res A.* 2003;66(1):176-183.
10. Erdogan O, Shafer DM, Taxel P, Freilich MA. A review of the association between osteoporosis and alveolar ridge augmentation. *Oral Surg Oral Med Oral Pathol Oral Radiol Endod.* 2007;104(6):738 e731-713.
11. Tsolaki IN, Madianos PN, Vrotsos JA. Outcomes of dental implants in osteoporotic patients. A literature review. *J Prosthodont.* 2009;18(4):309-323.
12. Namkung-Matthai H, Appleyard R, Jansen J, et al. Osteoporosis influences the early period of fracture healing in a rat osteoporotic model. *Bone.* 2001;28(1):80-86.
13. Kim SY, Kim SG, Lim SC, Bae CS. Effects on bone formation in ovariectomized rats after implantation of tooth ash and plaster of Paris mixture. *J Oral Maxillofac Surg.* 2004;62(7):852-857.
14. Shimizu M, Furuya R, Kawawa T, Sasaki T. Bone wound healing after maxillary molar extraction in ovariectomized aged rats: quantitative backscattered electron image analysis. *Anat Rec.* 2000;259(1):76-85.
15. Teofilo JM, Brentegani LG, Lamano-Carvalho TL. Bone healing in osteoporotic female rats following intra-alveolar grafting of bioactive glass. *Arch Oral Biol.* 2004;49(9):755-762.
16. Chen CH, Wang L, Serdar Tulu U, et al. An osteopenic/osteoporotic phenotype delays alveolar bone repair. *Bone.* 2018;112:212-219.
17. Salvi GE, Bosshardt DD, Lang NP, et al. Temporal sequence of hard and soft tissue healing around titanium dental implants. *Periodontol 2000.* 2015;68(1):135-152.
18. Agarwal R, Garcia AJ. Biomaterial strategies for engineering implants for enhanced osseointegration and bone repair. *Adv Drug Deliv Rev.* 2015;94:53-62.
19. Gao Y, Zou S, Liu X, Bao C, Hu J. The effect of surface immobilized bisphosphonates on the fixation of hydroxyapatite-coated titanium implants in ovariectomized rats. *Biomaterials.* 2009;30(9):1790-1796.

20. Vidigal GM, Jr., Groisman M, Gregorio LH, Soares Gde A. Osseointegration of titanium alloy and HA-coated implants in healthy and ovariectomized animals: a histomorphometric study. *Clin Oral Implants Res.* 2009;20(11):1272-1277.
21. Mardas N, Schwarz F, Petrie A, Hakimi AR, Donos N. The effect of SLActive surface in guided bone formation in osteoporotic-like conditions. *Clin Oral Implants Res.* 2011;22(4):406-415.
22. Qi M, Hu J, Li J, et al. Effect of zoledronate acid treatment on osseointegration and fixation of implants in autologous iliac bone grafts in ovariectomized rabbits. *Bone.* 2012;50(1):119-127.
23. Yang G, Song L, Guo C, Zhao S, Liu L, He F. Bone responses to simvastatin-loaded porous implant surfaces in an ovariectomized model. *Int J Oral Maxillofac Implants.* 2012;27(2):369-374.
24. Alghamdi HS, Bosco R, van den Beucken JJ, Walboomers XF, Jansen JA. Osteogenicity of titanium implants coated with calcium phosphate or collagen type-I in osteoporotic rats. *Biomaterials.* 2013;34(15):3747-3757.
25. Fraser D, Mendonca G, Sartori E, Funkenbusch P, Ercoli C, Meirelles L. Bone response to porous tantalum implants in a gap-healing model. *Clin Oral Implants Res.* 2019;30(2):156-168.
26. Cochran DL, Nummikoski PV, Higginbottom FL, Hermann JS, Makins SR, Buser D. Evaluation of an endosseous titanium implant with a sandblasted and acid-etched surface in the canine mandible: radiographic results. *Clin Oral Implants Res.* 1996;7(3):240-252.
27. Zhao G, Raines AL, Wieland M, Schwartz Z, Boyan BD. Requirement for both micron- and submicron scale structure for synergistic responses of osteoblasts to substrate surface energy and topography. *Biomaterials.* 2007;28(18):2821-2829.
28. Gittens RA, Olivares-Navarrete R, Schwartz Z, Boyan BD. Implant osseointegration and the role of microroughness and nanostructures: lessons for spine implants. *Acta Biomater.* 2014;10(8):3363-3371.
29. Mendonca DB, Miguez PA, Mendonca G, Yamauchi M, Aragao FJ, Cooper LF. Titanium surface topography affects collagen biosynthesis of adherent cells. *Bone.* 2011;49(3):463-472.
30. Mendonca G, Mendonca DB, Aragao FJ, Cooper LF. Advancing dental implant surface technology--from micron- to nanotopography. *Biomaterials.* 2008;29(28):3822-3835.

31. Wall I, Donos N, Carlqvist K, Jones F, Brett P. Modified titanium surfaces promote accelerated osteogenic differentiation of mesenchymal stromal cells in vitro. *Bone.* 2009;45(1):17-26.
32. Khan MR, Donos N, Salih V, Brett PM. The enhanced modulation of key bone matrix components by modified Titanium implant surfaces. *Bone.* 2012;50(1):1-8.
33. Calciolari E, Hamlet S, Ivanovski S, Donos N. Pro-osteogenic properties of hydrophilic and hydrophobic titanium surfaces: Crosstalk between signalling pathways in in vivo models. *J Periodontal Res.* 2018;53(4):598-609.
34. Jiang P, Liang J, Song R, et al. Effect of Octacalcium-Phosphate-Modified Micro/Nanostructured Titania Surfaces on Osteoblast Response. *ACS Appl Mater Interfaces.* 2015;7(26):14384-14396.
35. Wang Z, Goh J, Das De S, et al. Efficacy of bone marrow-derived stem cells in strengthening osteoporotic bone in a rabbit model. *Tissue Eng.* 2006;12(7):1753-1761.
36. Sanghani-Kerai A, Osagie-Clouard L, Blunn G, Coathup M. The influence of age and osteoporosis on bone marrow stem cells from rats. *Bone Joint Res.* 2018;7(4):289-297.
37. Chen Q, Shou P, Zheng C, et al. Fate decision of mesenchymal stem cells: adipocytes or osteoblasts? *Cell Death Differ.* 2016;23(7):1128-1139.
38. Pino AM, Rosen CJ, Rodriguez JP. In osteoporosis, differentiation of mesenchymal stem cells (MSCs) improves bone marrow adipogenesis. *Biol Res.* 2012;45(3):279-287.
39. Yuan JS, Reed A, Chen F, Stewart CN, Jr. Statistical analysis of real-time PCR data. *BMC Bioinformatics.* 2006;7:85.
40. Wescott DC, Pinkerton MN, Gaffey BJ, Beggs KT, Milne TJ, Meikle MC. Osteogenic gene expression by human periodontal ligament cells under cyclic tension. *J Dent Res.* 2007;86(12):1212-1216.
41. Wennerberg A, Albrektsson T. Effects of titanium surface topography on bone integration: a systematic review. *Clin Oral Implants Res.* 2009;20 Suppl 4:172-184.
42. Lang NP, Salvi GE, Huynh-Ba G, Ivanovski S, Donos N, Bosshardt DD. Early osseointegration to hydrophilic and hydrophobic implant surfaces in humans. *Clin Oral Implants Res.* 2011;22(4):349-356.

43. Sartoretto SC, Alves AT, Resende RF, Calasans-Maia J, Granjeiro JM, Calasans-Maia MD. Early osseointegration driven by the surface chemistry and wettability of dental implants. *J Appl Oral Sci.* 2015;23(3):279-287.
44. Mardas N, Busetti J, de Figueiredo JA, Mezzomo LA, Scarparo RK, Donos N. Guided bone regeneration in osteoporotic conditions following treatment with zoledronic acid. *Clin Oral Implants Res.* 2017;28(3):362-371.
45. Arioka M, Zhang X, Li Z, et al. Osteoporotic Changes in the Periodontium Impair Alveolar Bone Healing. *Journal of dental research.* 2019;98(4):450-458.
46. Chai YC, Carlier A, Bolander J, et al. Current views on calcium phosphate osteogenicity and the translation into effective bone regeneration strategies. *Acta Biomater.* 2012;8(11):3876-3887.
47. Barradas AM, Fernandes HA, Groen N, et al. A calcium-induced signaling cascade leading to osteogenic differentiation of human bone marrow-derived mesenchymal stromal cells. *Biomaterials.* 2012;33(11):3205-3215.
48. Cochran DL, Schenk RK, Lussi A, Higginbottom FL, Buser D. Bone response to unloaded and loaded titanium implants with a sandblasted and acid-etched surface: a histometric study in the canine mandible. *J Biomed Mater Res.* 1998;40(1):1-11.
49. Kokubo T, Takadama H. How useful is SBF in predicting in vivo bone bioactivity? *Biomaterials.* 2006;27(15):2907-2915.
50. Peng F, Yu X, Wei M. In vitro cell performance on hydroxyapatite particles/poly(L-lactic acid) nanofibrous scaffolds with an excellent particle along nanofiber orientation. *Acta Biomater.* 2011;7(6):2585-2592.
51. Gardin C, Ferroni L, Bressan E, et al. Adult stem cells properties in terms of commitment, aging and biological safety of grit-blasted and Acid-etched ti dental implants surfaces. *Int J Mol Cell Med.* 2014;3(4):225-236.
52. Leung KS, Fung KP, Sher AH, Li CK, Lee KM. Plasma bone-specific alkaline phosphatase as an indicator of osteoblastic activity. *J Bone Joint Surg Br.* 1993;75(2):288-292.
53. Mavrogenis AF, Dimitriou R, Parvizi J, Babis GC. Biology of implant osseointegration. *J Musculoskelet Neuronal Interact.* 2009;9(2):61-71.
54. Bosshardt DD, Salvi GE, Huynh-Ba G, Ivanovski S, Donos N, Lang NP. The role of bone debris in early healing adjacent to hydrophilic and hydrophobic implant surfaces in man. *Clin Oral Implants Res.* 2011;22(4):357-364.

55. Du D, Zhou Z, Zhu L, et al. TNF-alpha suppresses osteogenic differentiation of MSCs by accelerating P2Y2 receptor in estrogen-deficiency induced osteoporosis. *Bone.* 2018;117:161-170.
56. Buser D, Broggini N, Wieland M, et al. Enhanced bone apposition to a chemically modified SLA titanium surface. *J Dent Res.* 2004;83(7):529-533.
57. Bornstein MM, Valderrama P, Jones AA, Wilson TG, Seibl R, Cochran DL. Bone apposition around two different sandblasted and acid-etched titanium implant surfaces: a histomorphometric study in canine mandibles. *Clin Oral Implants Res.* 2008;19(3):233-241.
58. Sartoretto SC, Alves A, Zarranz L, Jorge MZ, Granjeiro JM, Calasans-Maia MD. Hydrophilic surface of Ti6Al4V-ELI alloy improves the early bone apposition of sheep tibia. *Clin Oral Implants Res.* 2017;28(8):893-901.
59. Feng JQ, Ward LM, Liu S, et al. Loss of DMP1 causes rickets and osteomalacia and identifies a role for osteocytes in mineral metabolism. *Nat Genet.* 2006;38(11):1310-1315.
60. Liu T, Wang J, Xie X, et al. DMP1 Ablation in the Rabbit Results in Mineralization Defects and Abnormalities in Haversian Canal/Osteon Microarchitecture. *J Bone Miner Res.* 2019;34(6):1115-1128.
61. Calciolari E, Donos N, Mardas N. Osteoporotic Animal Models of Bone Healing: Advantages and Pitfalls. *J Invest Surg.* 2017;30(5):342-350.

## Figures and Legend

**Figure 1.** Two- and three-dimensional reconstructed images of OVX mice model 3 months post-surgery obtained by Nano CT scanning.

**Figure 2.** One cpTi grade IV implant (diameter 0.7 mm and length 8mm) prepared with a hydrophobic (SAE) (left) and one with hydrophilic (SAE-HD) (right) surface was placed in each femur.

**Figure 3 A and B.** Calcium and Phosphorus % Atomic content measured by EDS on the surface of the implant (n=5 animals and n=6 measurements/sample). The results are expressed as the mean ± SD; * represents statistically significant difference ($p<0.05$).

**Figure 4.** Representative Nano CT 3D reconstruction. New bone tissue and the entire trabecular bone around implants are represented by yellow and green, respectively. SAE-HD and SAE implants at 14 days (A, B, C, and D) and 28 days (E, F, G, and H) after implant placement.

**Figure 5 A.** Quantification of BV obtained from Nano CT analyses calculated as a percentage of the total implant perimeter. Results are shown as mean percentages ± standard deviation in the SAE and SAE-HD groups, 14 and 28 days after implant placement. Statistically significant differences are indicated as follows: 14 days: * p=0.0001, ** p= 0.0120, ***p=0.0001, **** p=0.0001; 28 days: ***** p=0.0001.

**Figure 5 B.** Quantification of BIC obtained from Nano CT analyses calculated as a percentage of the total implant perimeter. Results are shown as mean percentages ± standard deviation in the SAE and SAE-HD groups, 14 and 28 days post-implantation. Statistically significant differences are indicated as follows: 14 days: * p=0.0026, ** p=0.0071; 28 days: ***p=0.0143, **** p=0.0196, ***** p=0.0132.

**Figure 6.** Representative photomicrographs of toluidine blue stained thin sections (original magnification at 2x, 4x and 10x) in bright field of SHAM (A, B, E, and F) and OVX (C, D, G and H) at 14 days and 28 days. Observe the presence of new bone formation and the contact between bone and implant for both groups. In Group SAE-HD at 28 days, see the presence of trabecular bone more compact and in a greater number than Group SAE at the same period, suggesting the acceleration of osseointegration.

**Figure 7.** BIC of histology analyses calculated as a percentage of the total implant perimeter. Results are shown as mean percentages ± standard error of the mean (SEM) in the SAE and SAE-HD groups, 14 and 28 days after implant placement. Statistically significant differences are indicated as follows: * p=0.0163 and ** p= 0.0238.

**Figure 8 A.** Relative gene expression level for early osteogenic genes: *Alp*, *Runx2*, and *Sp7*. Total RNA was isolated on days 3 and 7. The results are shown in the relative expression for the SAE Day 3 (Method $2^{-\Delta\Delta Ct}$), n = 5 per group.

**Figure 8 B** Relative gene expression level for late osteogenic genes: *Sost*, *Bsp*, and *Ocn*. Total RNA was isolated on days 3 and 7. The results are shown in the relative expression for the SAE Day 3 (Method $2^{-\Delta\Delta Ct}$), n = 5 per group.

**Figure 8 C**. Relative gene expression level for pro-inflammatory (*IL-1β* and *Tnf-α*) and anti-inflammatory genes (*IL-10* and *Nos2*). Total RNA was isolated on days 3 and 7. The results are shown in the relative expression for the SAE day 3 (Method $2^{-\Delta\Delta Ct}$), n = 5 per group.

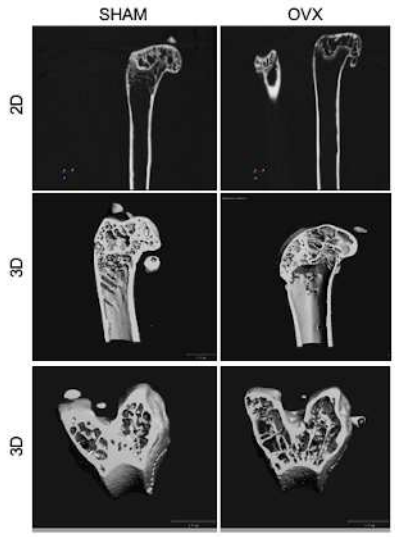


jre_12827_f1.tiff


jre_12827_f2.tiff

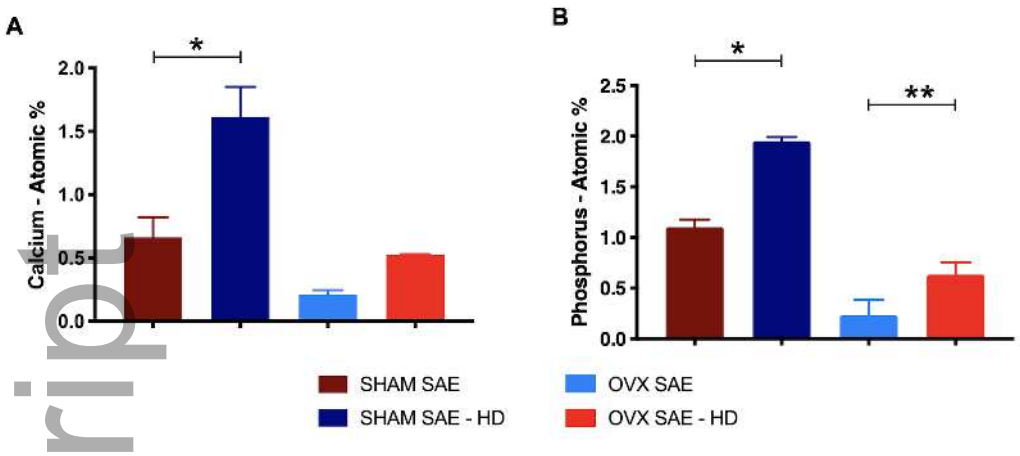


jre_12827_f3.tiff

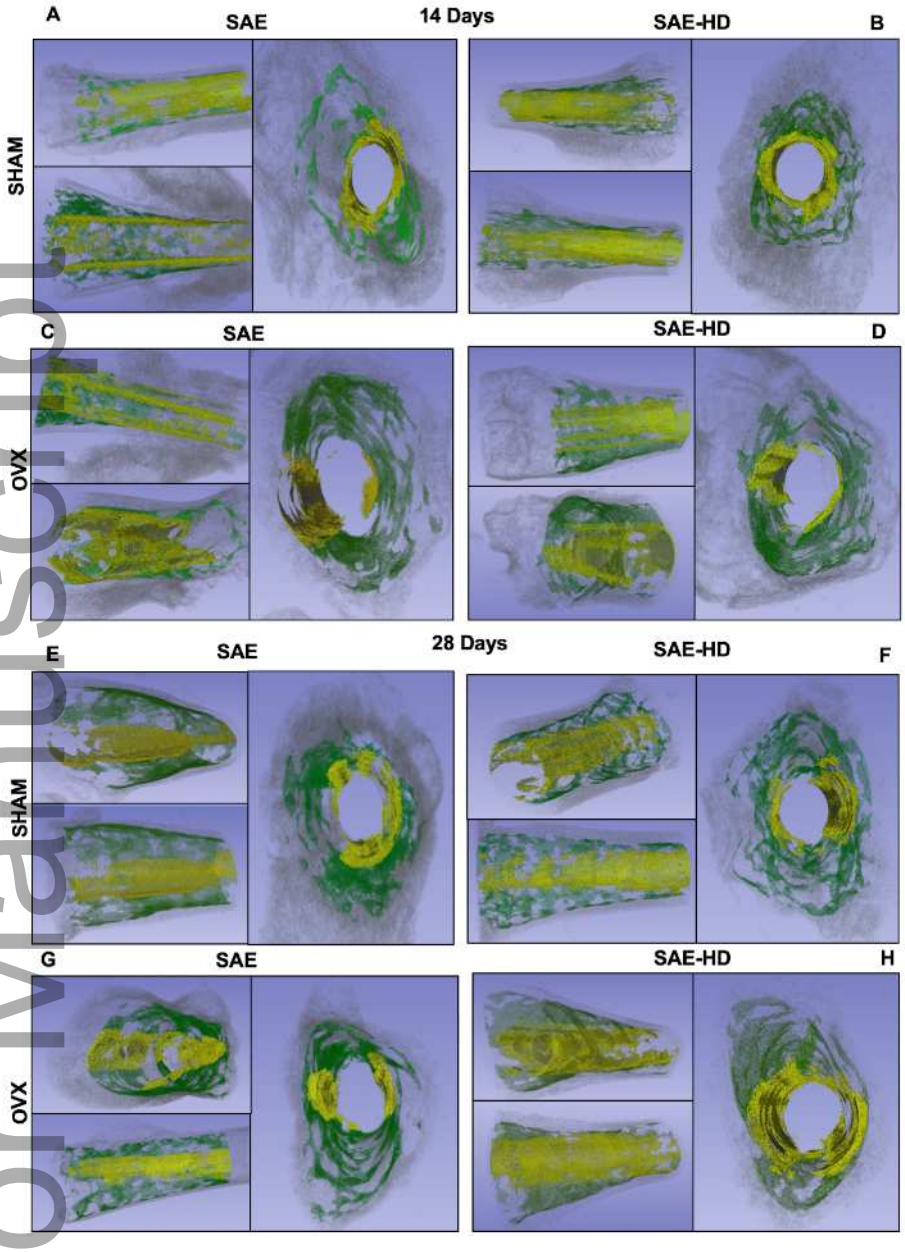


jre_12827_f4.tiff

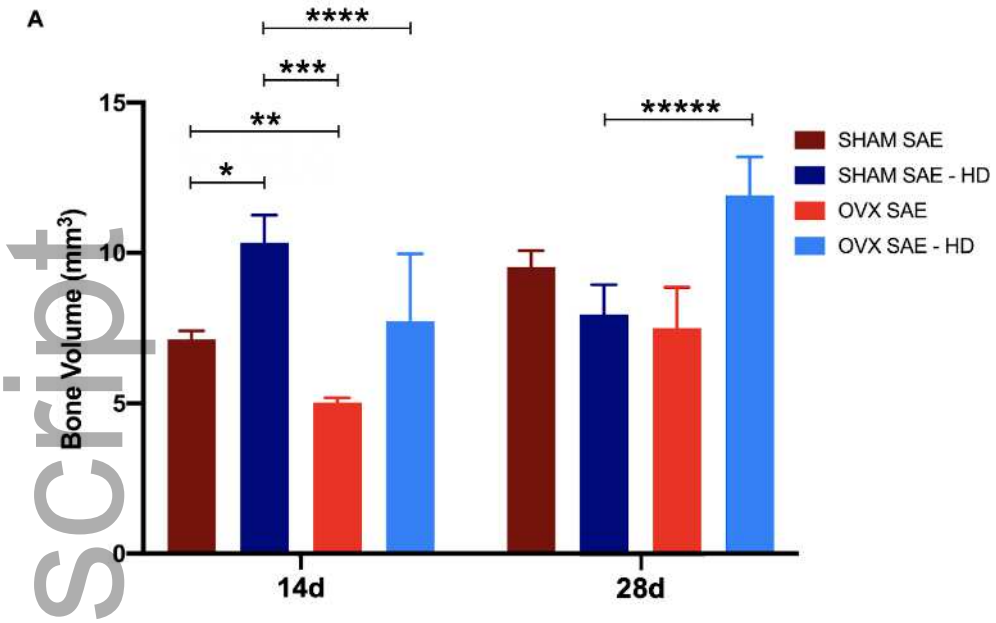


jre_12827_f5a.tiff

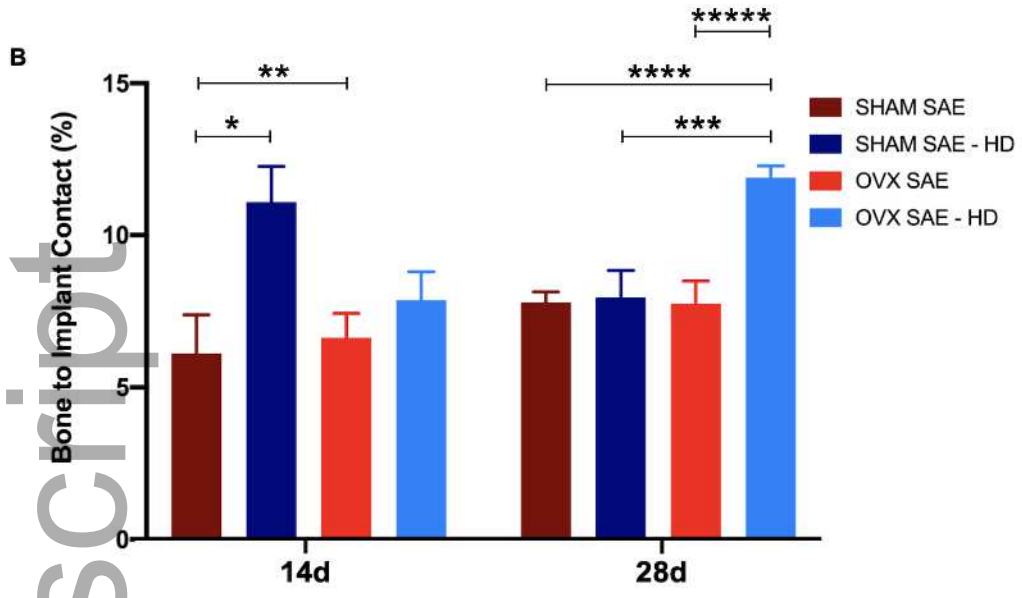


jre_12827_f5b.tiff

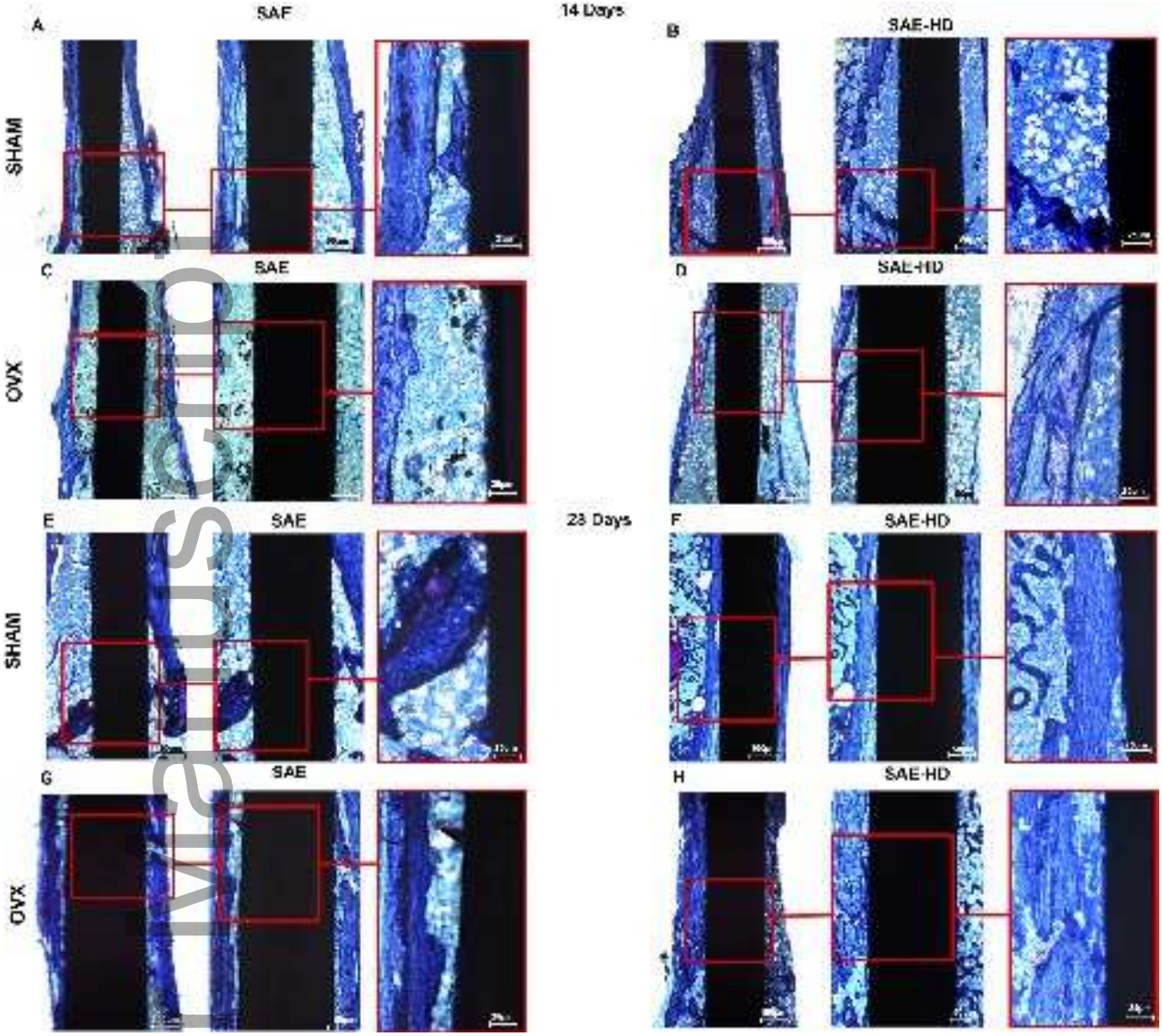


jre_12827_f6.tiff

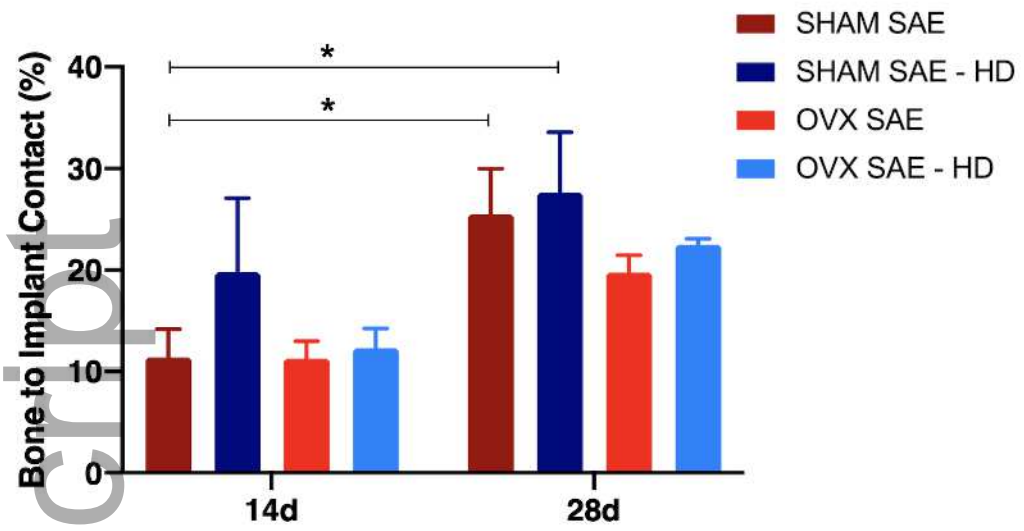


jre_12827_f7.tiff

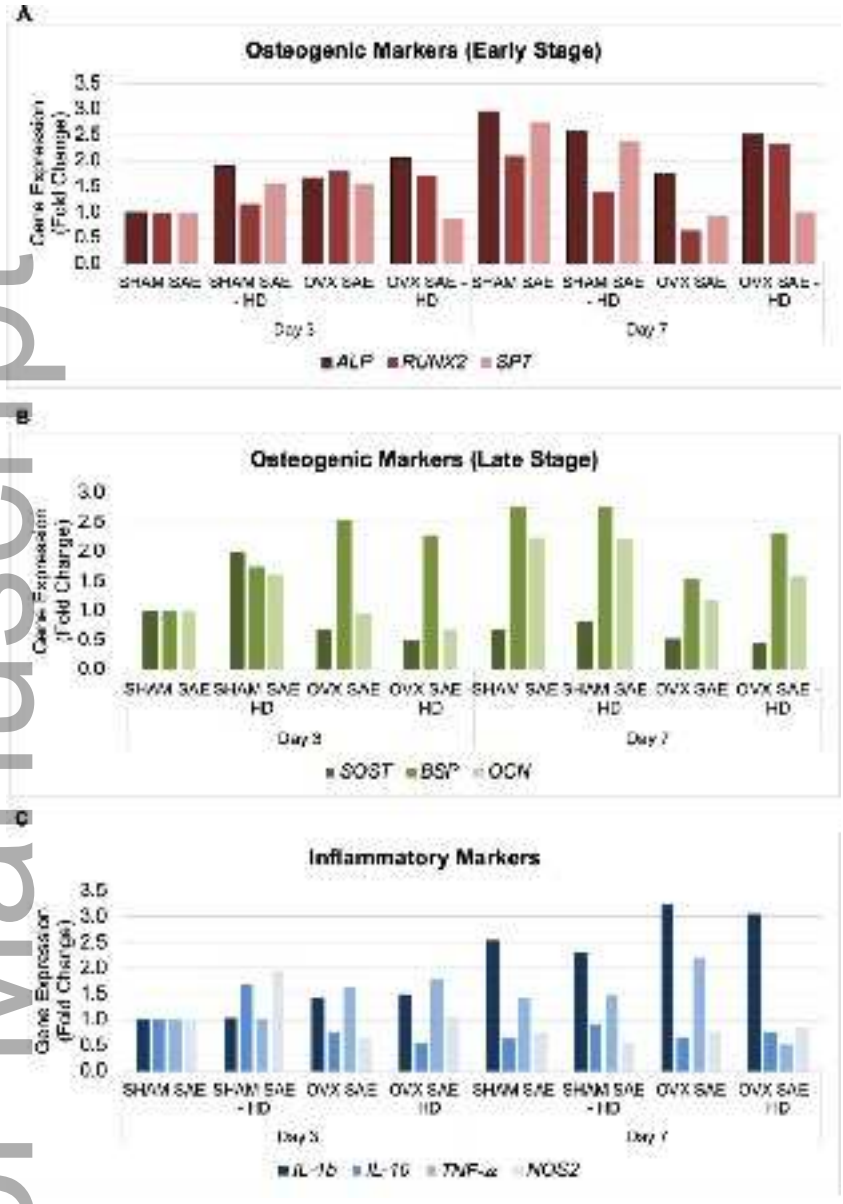


jre_12827_f8.tiff